Proc. Natl. Acad. Sci. USA
Vol. 93, pp. 3221–3226, April 1996
Biochemistry

Protein–RNA interactions in the active center of transcription elongation complex

VADIM MARKOVTSOV*, ARKADY MUSTAEV, AND ALEX GOLDFARB†

The Public Health Research Institute, New York, NY 10016

Communicated by Michael J. Chamberlin, University of California, Berkeley, CA, December 15, 1995 (received for review September 25, 1995)

ABSTRACT **By using a crosslinkable probe incorporated into the 3′ terminus of nascent transcript, three sites were mapped in *Escherichia coli* RNA polymerase that are contacted by the RNA in the productive elongation complex. Two of these sites are in the β subunit and one is in the β′ subunit. During elongation, the transcription complex occasionally undergoes an arrest whereby it can neither extend nor release the RNA transcript. It is demonstrated that in an arrested complex, the three contacts of RNA 3′ terminus are lost, while a new β′ subunit contact becomes prominent. Thus, elongation arrest appears to involve the disengagement of the bulk of the active center from the 3′ terminus of RNA and the transfer of the terminus into a new protein environment.**

The multisubunit cellular DNA-dependent RNA polymerase (RNAP) is the principal enzyme of gene expression and the target for genetic regulatory mechanisms. The principal structural determinants of RNAP basic activity are highly conserved in evolution as is evident from sequence homology of the two largest RNAP subunits throughout eubacterial, archaebacterial, and eukaryotic kingdoms (1–4). The evolutionary conservation of the general architecture of RNAP molecule has been confirmed by low-resolution structural analysis (5–7). The best characterized RNAP is that from *Escherichia coli*. Its catalytic core component ($\alpha_2\beta\beta'$) is composed of three types of subunit, α (329 amino acid residues), β (1342 residues), and β′ (1407 residues). The RNAP holoenzyme ($\alpha_2\beta\beta'\sigma$) carries in addition one of several σ factors required for specific promoter recognition.

To identify subunit sites involved in the formation of the active center, crosslinkable analogs of RNAP substrates have been used. Mapping of the contact sites by using probes carrying a reactive group at the 5′ side of the priming NTP helped to pinpoint several sites participating in the 5′ face of the active center. They include the evolutionarily invariant residues Lys^{1065} and His^{1237} near the C terminus of the β subunit (8–10), a region in the middle of β between Asp^{516} and Arg^{540} where many mutations of resistance to rifampicin are found (11), and a conserved motif of the initiation subunit σ^{70} (12).

Mapping of the protein sites facing the 3′ terminus of RNA is predicated by one's ability to incorporate a crosslinkable probe into the transcript terminus. In a previous communication, this laboratory (13) used a chain-terminating photocrosslinkable analog of AMP, 8-N_3-AMP carrying the reactive group at the purine base ring to identify a crosslinking site between Met^{932} and Trp^{1020} in the β′ subunit. Here we use a pyrimidine nucleotide carrying a base ring probe, 4-S-UMP, to identify three additional RNAP sites contacting the 3′ end of RNA in the elongating ternary complex.

Mapping of the RNA–protein contacts is particularly interesting in view of a recent model of transcription elongation that postulates a substantial degree of relative movement of parts within the advancing complex (refs. 14–20; for review, see refs. 21–23). During elongation, the advancing complex alternates between monotonic movement and cycles of conformational rearrangements resembling the movements of an inchworm (17). During inchworming, the front-end domain of RNAP appears to stall while the RNA chain continues to grow, and the ternary complex behaves as if it accumulates internal strain. The straining of the complex may lead to two alternative outcomes: a forward leap of the front-end domain over several base pairs or a collapse of the complex into the arrested (dead-end) conformation in which RNAP can neither continue nor release the transcript (15, 17, 20). Elongation arrest is a side pathway in the termination process (20) and is believed to be the biological justification for the internal transcript cleavage induced by the GreB protein (15) and its eukaryotic analog SII (24–27). The cleavage lifts the arrest by removing a 3′-proximal fragment of RNA and enabling RNA polymerase to retry navigating through a potentially arresting site. Thus, understanding of elongation arrest is important for deciphering the molecular mechanisms of elongation and termination.

It has been suggested that elongation arrest involves disengagement of the active center from the 3′ terminus of the transcript (15, 20, 21). Accordingly, we compared the crosslinking contacts of RNA terminus in a productive and arrested complexes and observed a profound difference consistent with the disengagement model.

MATERIALS AND METHODS

Reagents. 4-S-UTP was synthesized from 4-S-UMP (Sigma) as described (28). RNAP carrying six-histidine tag at the C terminus of the β′ subunit (His-tagged RNAP) was obtained according to Kashlev and coworkers (17). Protein cleavage reagents were from Sigma.

Preparation of Ternary Complexes. The productive EC^{27} complex was prepared by "walking" of His-tag RNA polymerase through T7A1 promoter DNA fragment essentially as described (20). Briefly, 2 μg (4 pmol) of the RNAP was incubated for 5 min with equimolar amount of the template and the resulting binary complex was immobilized on 10 μl of Ni-NTA agarose followed by the addition of CpApUpC (to 5 μM), ATP (to 20 μM), and GTP (to 20 μM). The resultant ternary complex carrying an 11-nt transcript was washed by repeated centrifugation of the resin beads and then extended to EC^{20} by adding 1 μM [α-P^{32}]ATP, 1 μM [α-P^{32}]GTP, and 1 μM [α-P^{32}]CTP (3000 Ci/mmol; 1 Ci = 37 GBq). Productive EC^{27} was synthesized by further extending the radiolabeled complex using appropriate unlabeled NTPs at 10 μM. The last step was a 5-min extension with ATP (10 μM) and 4-S-UTP (100 μM) carried out at 0°C to prevent dead-end formation followed by removal of unincorporated NTPs by brief (5–7 sec)

The publication costs of this article were defrayed in part by page charge payment. This article must therefore be hereby marked "*advertisement*" in accordance with 18 U.S.C. §1734 solely to indicate this fact.

Abbreviations: RNAP, RNA polymerase; TNCBA, 2-nitro-5-thiocyanobenzoic acid.

*Present address: Department of Chemistry, Moscow State University, Moscow, Russia.
†To whom reprint requests should be addressed.

repeated washing and centrifugation using ice-cold buffer. "Chase" of EC^{27} into EC^{34} was achieved by adding the mixture of 10 μM ATP, 10 μM GTP, and 10 μM CTP followed by a 3-min incubation at room temperature. The process was stopped by adding equal volume of sample buffer containing 8 M urea to the reaction mixture.

The arrested (dead-end) EC^{27} was prepared from the productive complex by a 1-h incubation at 37°C in the standard buffer (17). The conversion was effectively stopped by placing the tubes back on ice. Control experiments have demonstrated that complexes remain productive during at least several hours of incubation at 0°C.

Electrophoretic analysis of RNA in the complexes was carried out in a 12% polyacrylamide gel in Tris/borate buffers system in the presence of 8 M urea as described (17).

UV-Crosslinking and Isolation of the Crosslinked Subunits. Samples were irradiated on ice for 20 min at 360 nm with a UV hand lamp UVGL-25 (Ultraviolet Products) placed on the top of an Eppendorf tube. The samples were treated with imidazole at 150 mM to remove the complexes from resin beads, and the supernatant material was fractionated by PAGE in a 4% polyacrylamide/SDS gel followed by autoradiography. The β or β′ subunits carrying radioactive RNA were excised from the gel and eluted by 3 vol of 0.2% SDS at 37°C for 1 h. The eluates were freeze-dried with a SpeedVac and redissolved then in water to the final concentration of 1–2% SDS.

Mapping of the Crosslinks. Partial and exhaustive degradation of the subunits by CNBr, 2-nitro-5-thiocyanobenzoic acid (TNCBA), and hydroxylamine was performed as described (8, 9, 13). The cleavage products were fractionated by SDS/PAGE with the indicated concentration of acrylamide. Electrophoresis was performed in Tris/glycine (29) or, where specifically indicated, in Tris/Tricine (30) buffer system.

RESULTS

RNA Crosslinking in Productive and Arrested Complexes. Ternary elongation complex in the T7A1 transcription unit carrying the 27-nt transcript (EC^{27}) has been previously shown to be predisposed to elongation arrest (dead-end formation) (17). In a preliminary experiment, we have found that EC^{27} carrying 4-S-UMP in the 3′ terminus is indistinguishable from the complex with common uridine in every respect including the rate of arrest (data not shown). Fig. 1*A* illustrates the kinetics of dead-end formation of the 4-S-UMP-carrying EC^{27} as determined by its ability to be "chased" into EC^{34} upon the addition of three NTPs. After 16 min of incubation at 37°C, more than 80% of the complex could not be chased. The conversion into dead-end is accompanied by a change in the pattern of crosslinking of the 3′-terminal 4-S-UMP upon UV-irradiation (Fig. 1*B*). The productive EC^{27} (0 min) displays approximately one-third of the total crosslinking in the β subunit. In the arrested EC^{27} (16 min), the crosslinking of β nearly disappears. The crosslinking of β′ increases 3- to 4-fold over the period of 1 h (Fig. 1*C*), i.e., continues to accumulate long after most of the complex has entered into the arrested state (Fig. 1*A*). This pattern of crosslinking was reproducible in several experiments.

Crosslinks in the β Subunit. To map the crosslinking sites, we employed the approach developed by Grachev *et al.* (9), which consists in partial chemical degradation of a subunit carrying the crosslinked adduct under single-hit conditions, i.e., when less than one cleavage per polypeptide occurs on average. Single-hit degradation yields two families of nested fragments: the C-terminal fragments and the N-terminal fragments. If the crosslinked radiolabeled adduct is located closer to one of the termini, the PAGE pattern of shorter radiolabeled peptide bands allows one to map the crosslink between two adjacent cleavage sites (see scheme in Fig. 2*A*). The technique is illustrated by a reference experiment (Fig. 2*B*, lane 8) that is a reproduction of a previously reported observation (9), i.e., the pattern resulting from single-hit CNBr degradation of the β subunit carrying a radiolabeled trinucleotide crosslinked to His^{1237} through a 5′-terminal link (symbolized by an open circle). The pattern of bands a to o in lane 8 represents the family of nested radiolabeled C-terminal fragments.

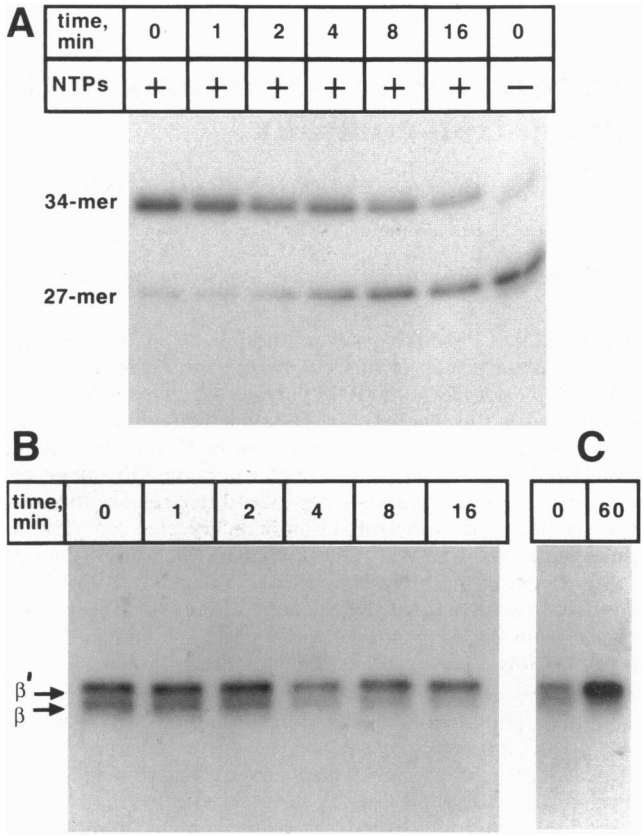

FIG. 1. Transition of EC^{27} from productive to arrested state. (*A*) Loss of "chaseability" of EC^{27} into EC^{34}. The autoradiogram of a 12% polyacrylamide gel with 8 M urea shows RNA made when EC^{27} (containing photocrosslinkable 3′-terminal 4-S-uridine) was incubated at 37°C for various intervals prior to the addition of three NTPs. Elongation of EC^{27} was carried out for 3 min at room temperature. (*B*) Crosslinking of RNA to β and β′ subunits. The autoradiogram of a 4% polyacrylamide/SDS gel showing the subunits crosslinked to RNA in EC^{27} incubated for the indicated times prior to irradiation. (*C*) Same as *B*, but the incubation was for 0 min and 60 min.

To map the crosslinking site(s) of the 3′-terminal probe in the productive EC^{27} (see Fig. 1), single-hit degradation was carried out for two incubation periods with CNBr (Fig. 2*B*, lanes 2 and 3). The pattern of radioactive bands partially matches that in the reference lane 8 (corrected for the increment of molecular weight due to the 27-nt adduct). The pattern in lanes 2 and 3 begins with fragment f while fragments a–e are not seen on the autoradiogram. The result indicates that the crosslink occurred between the breakpoints of fragments f and e, i.e., Pro^{1086} and Met^{1107}, as symbolized by a solid box in the scheme of Fig. 2*A*. The location of the crosslink was further narrowed down by single-hit cleavage at Asn-Gly with NH_2OH (lanes 6 and 7). The pattern of the labeled bands p, q, and r is consistent with Asn-Gly sites at the C terminus. The shortest labeled peptide is p, testifying that the crosslink is located distally of Gly^{1091}. Single-hit cleavage at Cys with TNCBA (lanes 4, 5) is consistent with the localization of the crosslink at the C-terminal fragment s. From these results, we conclude that the crosslinking site is located within the 17-amino acid segment Gly^{1091}–Met^{1107}.

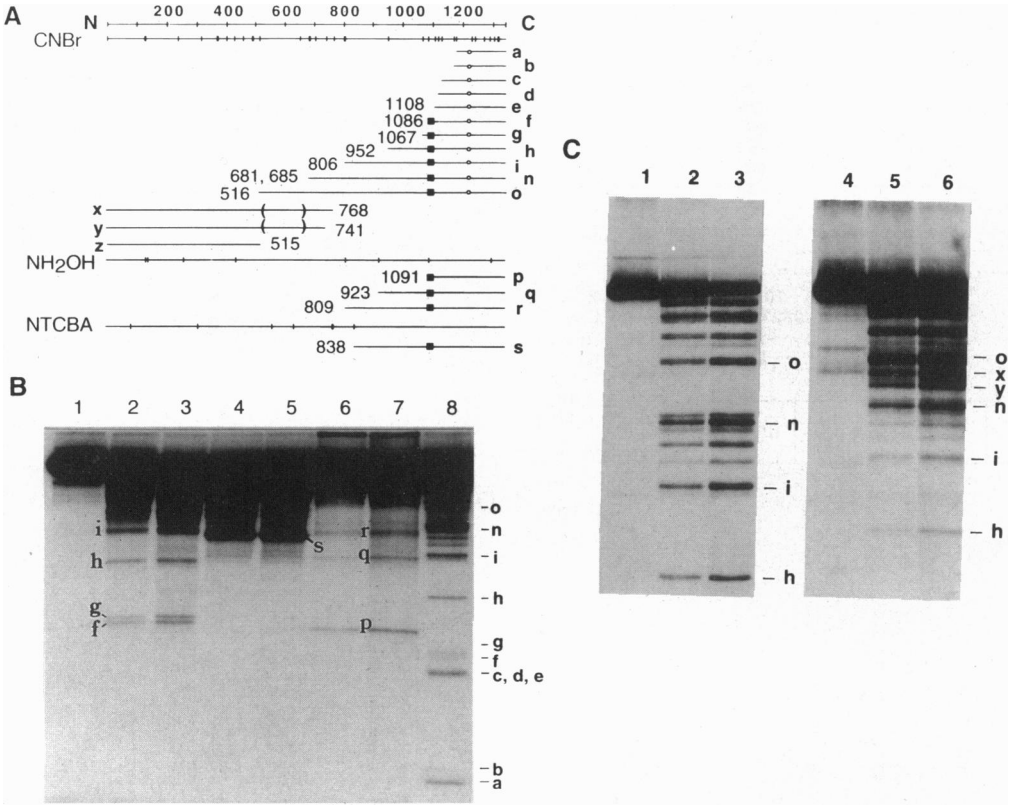

FIG. 2. Mapping of the crosslinking sites in β. (*A*) Chemical degradation map of the β subunit. Horizontal line at the top symbolizes the 1342-amino acid β polypeptide. Lines with vertical bars represent the cleavage maps with CNBr, NH_2OH, and TNCBA, which cleave at Met, Cys, and Asn-Gly, respectively. Lettered lines represent degradation products discussed in the text. Terminal residues of the cleavage products are indicated by numbers. The open circle indicates the position of 5′-terminal crosslink to His^{1237} (9), which was used as reference. The solid box symbolizes the C-proximal 3′-terminal crosslink identified in this work. Parentheses on the fragments x and y delineate the areas of the N-proximal 3′-terminal crosslink. (*B*) An autoradiogram of a gradient SDS gel (10–20% polyacrylamide) showing products of degradation of the β subunit from irradiated EC^{27}. Lanes: 1, untreated material; 2 and 3, CNBr for 5 and 10 min, respectively; 4 and 5, TNCBA for 15 and 30 min; 6 and 7, hydroxylamine for 30 and 60 min; 8, reference, CNBr cleavage of β labeled at His^{1237}. Lettered products correspond to fragments in *A*. (*C*) Fractionation at a lower percentage of acrylamide (8%) to resolve longer products of CNBr degradation. Lanes: 1–3, His^{1237}-modified reference; 4–6, experimental material. Treatments: 0 min, lanes 1 and 4; 5 min, lanes 2 and 5; 10 min, lanes 3 and 6.

Fig. 2*C* shows the separation of the CNBr cleavage products at a longer PAGE run permitting analysis of high molecular weight fragments. One can see a striking difference between the cleavage patterns of the reference (trinucleotide adduct at His^{1237}, lanes 2 and 3) and the experimental sample representing β with RNA crosslinked in EC^{27} (lanes 5 and 6). In the EC^{27} pattern, two prominent new bands x and y appear, and the relative intensity of band n (compared to bands i and h) is drastically increased. From this we infer that in EC^{27}, RNA is crosslinked to β at two alternative locations, one close to the C terminus as established above (solid box in Fig. 2*A*) and the other more proximal to the N terminus as indicated by parenthesis on fragments x and y in Fig. 2*A*. The argument behind this conclusion is as follows.

Fragments x and y are shorter than fragment o and longer than fragment n and cannot come from the C-terminal family since there are no appropriate cleavage sites between the breakpoints of o and n. Measured from the N terminus, the lengths of n and o project to positions ≈660 and 827, respectively (indicated by down-pointed arrows in Fig. 2*A*). Thus, x and y apparently result from CNBr cleavage at Met^{768} and Met^{741}, respectively. The fact that the relative intensity of n is about twice as high in the experimental sample (lanes 5 and 6) as in the reference (lanes 2 and 3) probably reflects overlapping of radiolabeled N- and C-terminal fragments of the same mobility. Thus, the N-proximal crosslink site should be to the left of the n projection around position ≈660 (presumably this is Met^{654}). The nearest upstream CNBr cleavage at Met^{515} should generate an N-terminal fragment z that would migrate between the C-terminal fragments i and h (537 and 391 amino acids, respectively). No such band is seen in lanes 5 and 6. Thus, fragment z does not carry the crosslinked RNA. We conclude that the N-proximal crosslinking site is located between the breakpoints of fragments z and y, i.e., between positions 515 and ≈660.

Crosslink in the β′ Subunit from Arrested EC^{27}. As is evident from Fig. 1 *B* and *C*, the conversion from the productive to the arrested complex is accompanied by the initial decrease in the RNA crosslinking to the β′ subunit followed by a significant subsequent raise of the crosslinking yield. Such kinetics suggests that RNA crosslinks to different sites in productive and arrested complexes. In this section we present the analysis of the crosslink from the arrested complex. The cleavage map of β′ is shown in Fig. 3*A*.

Fig. 3*B* shows the results of exhaustive digestion with TNCBA that cleaves near Cys residues. This reagent cleaves β′ preferentially at the distal Cys^{895} and Cys^{898} (13). As can be seen, the radioactivity is recovered in a 69-kDa peptide (fragment a) testifying that the crosslink(s) occurs distally of Cys^{898}. The crosslink was further localized by using single-hit cleavage at Met residues with CNBr (Fig. 3*C*, lanes 2 and 3). As a reference, an overexposed autoradiogram of single-hit cleavage with TNCBA is presented in lanes 4 and 5 displaying characteristic pattern of C-terminal fragments a–i. From the comparison of the CNBr and TNCBA patterns, it can be inferred that the three shortest products seen in lanes 2 and 3

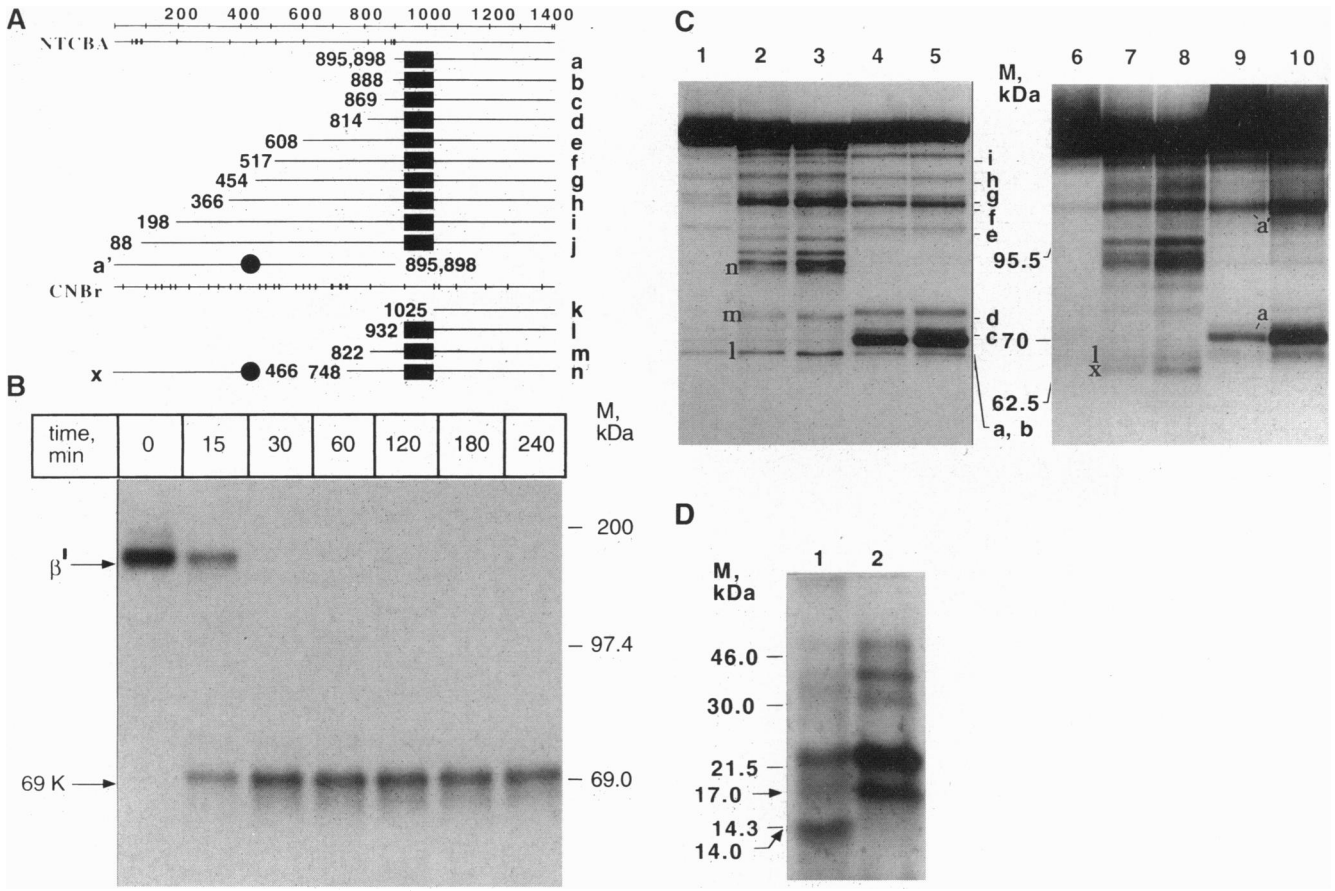

FIG. 3. Mapping of the crosslinking sites in β'. (*A*) Chemical degradation map of the β' subunit. Horizontal line at the top symbolizes the 1407-amino acid β' polypeptide. Lines with vertical bars represent the cleavage maps with TNCBA and CNBr. Lettered lines represent degradation products discussed in the text. Terminal residues of the cleavage products are indicated by numbers. The solid circle and the solid box indicate the position of crosslinks identified in this work. (*B*) An autoradiogram of an SDS gel (10% polyacrylamide) showing exhaustive TNCBA degradation of the β' subunit from irradiated EC[27]. (*C*) Partial cleavage of the β' crosslinked within the arrested (lanes 1–5) or productive (lanes 6–10) EC[27]. Treatments: untreated material, lanes 1 and 6; CNBr, lanes 2 and 3 for 5 min and lanes 7 and 8 for 10 min); TNCBA, lanes 4 and 5 for 15 min and lanes 9 and 10 for 30 min. Productive complex here means freshly prepared EC[27] irradiated without prior incubation at 37°C. Arrested complex was obtained from productive EC[27] by 60-min incubation at 37°C. (*D*) Exhaustive CNBr degradation of β' crosslinked in the productive (lane 1) and arrested (lane 2) EC[27]. Fractionation in a 16% polyacrylamide Tris/Tricine gel.

are the C-terminal nested Met fragments l, m, and n. However, fragment k that should result from the next cleavage downstream is not seen. Thus, the crosslink is positioned between the breakpoints of l and k, i.e., Arg^{933} and Met^{1025}. This conclusion is corroborated by the results of exhaustive exposure to CNBr (Fig. 3*D*, lane 2). Although such treatment does not degrade the material completely, it allows one to identify the shortest ≈17-kDa Met fragment carrying the crosslinked RNA, which is consistent with the localization of the crosslink between Met^{932} and Met^{1025}.

Crosslink in the β' Subunit from Productive EC[27]. The crosslinked β' subunit from the productive EC[27] displays the pattern of cleavage consistent with two crosslinking sites: the site characteristic of the arrested state mapped in the preceding section and another additional site. This is evident from the results of exhaustive CNBr digestion (Fig. 3*D*, lane 1) that yields three prominent radioactive bands, only two of which are shared with the β' from the arrested complex (lane 2). The shortest Met fragment specific for the productive complex has an apparent molecular mass of 14 kDa.

There are at least four Met–Met segments in β' with the molecular mass of ≈14 kDa that could carry the crosslink specific for the productive complex (see Fig. 3*A*). To map the crosslink precisely, we used the single-hit cleavage conditions that yields two sets of C- and N-terminal fragments (see above). Cleavage of the crosslinked β' from the productive complex with TNCBA under single-hit conditions yields two predominant bands reflecting preferential degradation at a single Cys site at positions 895 and 898 (Fig. 3*C*, lanes 9 and 10). The C-terminal fragment a apparently carries the previously identified crosslink. The productive complex-specific crosslink is contained within the N-terminal fragment a'. For its fine mapping, we employed the single-hit exposure to CNBr. (Fig. 3*C*, lanes 7 and 8). The shortest resultant labeled Met fragment x migrates slightly ahead of the C-terminal fragment I. It is, however, is too long to result from the next distal Met^{1025} (fragment k). Thus, x is an N-terminal fragment, apparently resulting from cleavage at Met^{466}. We conclude that the β' RNA crosslink specific for the productive complex occurs between Met^{400} and Ala^{467}, as indicated by the solid circle in Fig. 3*A*.

DISCUSSION

Anatomy of the Active Center. The four regions of protein contact with the 3' terminus of RNA identified in this work are shown on the map of the β and β' subunits in Fig. 4. The crosslink that accumulates in the arrested state (Met^{932}–Met^{1025} in β') has been characterized (13). The other three crosslinks specific for the productive complex are newly identified.

The proximal crosslinking area in β (residues 515 to ≈660) is distinguished by the location of the two principal regions of rifampicin-resistant mutations, termed rifampicin clusters I

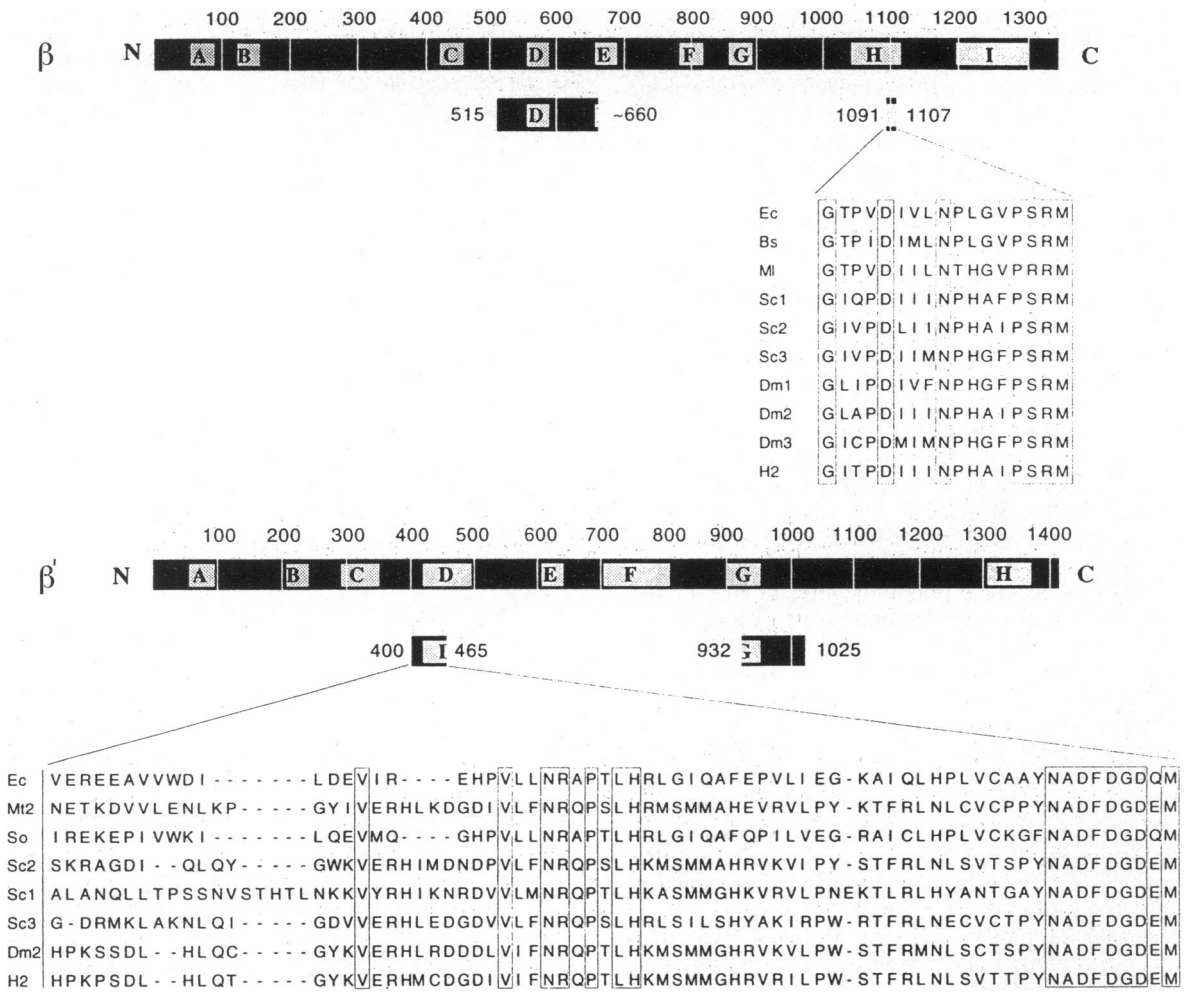

FIG. 4. Alignment of the newly found affinity labeled regions in the *E. coli* RNAP β and β′ subunits with those from other organisms. Evolutionarily conserved segments of β and β′ are shaded gray and designated by uppercase letters according to Sweetser *et al.* (1). EC, *E. coli*; Bs, *Bacillus subtilis*; Ml, *Mycobacterium leprae*; Mt2, *Methanobacterium thermoautotrophicum*; So, *S. oleracea* chloroplast; Sc1, *Saccharomyces cerevisiae* polymerase I; Sc2, *S. cerevisiae* polymerase II; Sc3, *S. cerevisiae* polymerase III; Dm1, *Drosophila melanogaster* polymerase I; Dm2, *D. melanogaster* polymerase II; Dm3, *D. melanogaster* polymerase III; H2, human polymerase II. Conserved sequences are boxed.

and II (amino acids 507–533 and 563–572, respectively) (31, 32). Between the two rifampicin clusters, mutants resistant to streptolydigin are found (32, 33). This area has been long suspected of involvement in the active center on the basis of the mechanism of action of the two antibiotics. Since rifampicin blocks the transition from initiation to elongation, it has been suggested that it acts by obstructing the transcript exit from the catalytic center (34). Streptolydigin inhibits extension of nascent RNA chains during initiation and elongation (35). The likely target of streptolydigin is either the binding of incoming NTP or the phosphodiester bond formation (36). It is reasonable to assume that both antibiotics bind near the active center, and consequently the regions of rifampicin-resistance and streptolydigin-resistance mutations are located close to the active center in the folded RNAP molecule. Recently, we found that a 5′-terminal reactive group placed on an initiating NTP crosslinks to the rifampicin cluster I (11). Our present results implicate some nearby locality in the 3′ face of the active site. Thus the segment 515–660 may participate in the two opposite sides of the catalytic pocket. Of course, this segment is long enough (145 amino acids) to participate in different elements of tertiary structure. Fine mapping of the 5′- and 3′-terminal crosslinks is currently in progress aimed at further dissection of this interesting region.

The distal crosslinking site in β (residues 1091–1107) is a part of the conserved region H. Previous studies have demonstrated that Lys^{1065} at the N side of region H crosslinks to the 5′-terminal probe on initiating NTPs (9, 10). Thus there are only ≈30 amino acids between the 5′ and 3′ contact sites in this area, which strongly suggests that region H participates in the catalytic pocket perhaps by forming a continuous element of the structure.

The proximal crosslinking region in β′ between residues 400 and 465 has not been previously implicated in any particular biochemical function. It is distinguished by the presence of the longest continuous evolutionarily conserved motif in RNA polymerase NADFDGD-M. It is tempting to speculate that the three Asp residues in this motif directly participate in the RNAP catalytic reaction by analogy with the adjacent aspartates that coordinate Mg^{2+} in the active center of DNA polymerase I, T7 RNA polymerase and human immunodeficiency virus reverse transcriptase (37). A recent study of mutants in this motif in eukaryotic RNA polymerase III supports the notion that this region is involved in the active site formation (38).

Mechanism of Elongation Arrest. The distal crosslink in the β′ subunit between Met^{932} and Met^{1025} becomes prominent upon prolonged incubation of the arrested complex. The ultimate yield of this crosslink observed after a 1-h incubation is several times higher than the overall crosslinking yield in the productive complex. In the freshly stopped elongation complex, the distal β′ crosslink is a minor species that probably

represents a small fraction of the arrested complexes that accumulates in the preparation during the first few minutes of incubation.

The distal crosslinking site in β′ has been identified by using a different 3′-terminal probe, 8-azido-adenine (13). The Met^{932}–Met^{1025} segment that harbors this crosslink carries ≈10 highly conserved amino acids at its N-proximal end (for sequence alignment, see figure 4 in ref. 13). We suggested that this motif may participate in the catalytic site. However, since 8-azido-adenine causes RNA chain termination, it was not possible to determine whether the complex that we analyzed was in a productive or arrested configuration. Our present results indicate that the crosslink in this area is not characteristic for the productive complex and, hence, may not represent the active site contact. Moreover, the distal crosslink accumulates ≈4 times more slowly that the rate with which the complex undergoes arrest. Thus the distal crosslink may represent a secondary event not immediately associated with the arrest—e.g., slow association of a loose RNA terminus with a high-affinity site on the protein.

The disappearance of the three crosslinks characteristic for the productive complex is a principal observation of this work. No conclusion can be made about the rate of loss of the proximal β′ crosslink because this process is masked by the slow accumulation of the distal β′ contact. However, the disappearance of the two β-subunit contacts corresponds to the arrest kinetics (Fig. 1 *A* and *B*). This result strongly indicates that at least in the complex studied (EC^{27}), the transition from the productive to the arrested state is accompanied by a major conformational rearrangement of the active center. It appears that in the arrested complex, the 3′ terminus of RNA has lost its principal contacts. The change of the protein environment of the 3′ terminus is consistent with the hypothesis that transcriptional arrest involves disengagement of the catalytic site from the 3′ terminus (15, 20, 21).

The disengagement model links transcriptional arrest with the phenomenon of transcript cleavage facilitated by the *E. coli* GreB protein (15) and the SII factor in eukaryotic polymerase II (25, 26). The cleavage is followed by the ejection of RNA 3′ fragment from the ternary complex and the restart of transcription from the newly generated 3′ terminus. The cleavage-and-restart reaction rescues the elongating complex from the arrested state.

Recently it was demonstrated that transcript cleavage is an intrinsic property of RNAP whereas the Gre and SII factors merely enhance this reaction (39, 40). For polymerase II, the cleavage was shown to occur through pyrophosphorolysis of an internal phosphodiester bond, which led to the suggestion that the cleavage is catalyzed by the disengaged active center (40). The model envisages that reengagement of the active center with the new 3′ terminus is coupled with the cleavage. Our present results add support to this model.

We thank E. Nudler for help and advice. This work was supported by Grant GM49242 from the National Institutes of Health.

1. Sweetser, D., Nonet, M. & Young, R. A. (1987) *Proc. Natl. Acad. Sci. USA* **84,** 1192–1196.
2. Falkenburg, D., Dworniczak, B., Faust, D. M. & Bautz, E. K. F. (1987) *J. Mol. Biol.* **195,** 929–937.
3. Berghofer, B., Krockel, L., Kortner, C., Truss, M., Schallenberg, J. & Klein, A. (1988) *Nucleic Acids Res.* **16,** 8113.
4. Pühler, G., Leffers, H., Gropp, F., Palm, P., Klenk, H.-P., Lottspeich, F., Garrett, R. A. & Zillig, W. (1989) *Proc. Natl. Acad. Sci. USA* **86,** 4569–4573.
5. Darst, S. A., Kubalek, E. W. & Kornberg, R. D. (1989) *Nature (London)* **340,** 730–732.
6. Darst, S. A., Edwards, A. M., Kubalek, E. W. & Kornberg, R. D. (1991) *Cell* **66,** 121–128.
7. Schultz, P., Celia, H., Riva, M., Sentenac, A. & Oudet, P. (1993) *EMBO J.* **12,** 2601–2607.
8. Grachev, M. A., Kolocheva, T. I., Lukhtanov, E. A. & Mustaev, A. A. (1987) *Eur. J. Biochem.* **163,** 113–121.
9. Grachev, M. A., Lukhtanov, E. A., Mustaev, A. A., Zaychikov, E. F., Abdukayumov, M. N., Rabinov, I. V., Richter, V. I., Skoblov, Y. S. & Chistyakov, P. G. (1989) *Eur. J. Biochem.* **180,** 577–585.
10. Mustaev, A., Kashlev, M., Lee, J., Polyakov, A., Lebedev, A., Zalenskaya, K., Grachev, M., Goldfarb, A. & Nikiforov, V. (1991) *J. Biol. Chem.* **266,** 23927–23931.
11. Severinov, K., Mustaev, A., Severinova, E., Kozlov, M., Darst, S. & Goldfarb, A. (1995) *J. Biol. Chem.* **270,** 29428–29432.
12. Severinov, K., Fenyo, D., Severinova, E., Mustaev, A., Chait, B. T., Goldfarb, A. & Darst, S. A. (1994) *J. Biol. Chem.* **269,** 20826–20828.
13. Borukhov, S., Lee, J. & Goldfarb, A. (1991) *J. Biol. Chem.* **266,** 23932–23935.
14. Krummel, B. & Chamberlin, M. J. (1992) *J. Mol. Biol.* **225,** 221–234.
15. Borukhov, S., Sagitov, V. & Goldfarb, A. (1993) *Cell* **72,** 459–466.
16. Mustaev, A., Kashlev, M., Zaychikov, E., Grachev, M. & Goldfarb, A. (1993) *J. Biol. Chem.* **268,** 19185–19187.
17. Nudler, E., Goldfarb, A. & Kashlev, M. (1994) *Science* **265,** 793–796.
18. Zaychikov, E., Denissova, L. & Heumann, H. (1995) *Proc. Natl. Acad. Sci. USA* **92,** 1739–1743.
19. Wang, D., Maier, T. I., Chan, C. L., Feng, G., Lee, D. N. & Landick, R. (1995) *Cell* **81,** 341–350.
20. Nudler, E., Kashlev, M., Nikiforov, V. & Goldfarb, A. (1995) *Cell* **81,** 351–357.
21. Chamberlin, M. (1994) *Harvey Lect.* **88,** 1–21.
22. Chan, C. L. & Landick, R. (1994) in *Transcription: Mechanisms and Regulation*, eds. Conavay, R. C. & Conaway, J. W. (Raven, New York), pp. 297–321.
23. Das, A. (1993) *Annu. Rev. Biochem.* **62,** 893–930.
24. Kerpolla, T. K. & Kane, C. M. (1991) *FASEB J.* **5,** 2833–2842.
25. Reines, D. (1992) *J. Biol. Chem.* **267,** 3795–3800.
26. Izban, M. G. & Luse, D. S. (1992) *Genes Dev.* **6,** 1342–1356.
27. Gu, W. & Reines, D. (1995) *J. Biol. Chem.* **270,** 11238–11244.
28. Hoard, D. & Ott, D. (1965) *J. Am. Chem. Soc.* **87,** 1785–1787.
29. Laemmli, U. K. (1970) *Nature (London)* **227,** 680–685.
30. Schagger, H. & von Jagow, G. (1987) *Anal. Biochem.* **166,** 368–379.
31. Jin, D. J. & Gross, C. A. (1988) *J. Mol. Biol.* **202,** 45–58.
32. Severinov, K., Soushko, M., Goldfarb, A. & Nikiforov, V. (1993) *J. Biol. Chem.* **268,** 14820–14825.
33. Heisler, L. M., Suzuki, H., Landick, R. & Gross, C. (1993) *J. Biol. Chem.* **268,** 25369–25375.
34. Mustaev, A., Zaychikov, E., Severinov, K., Kashlev, M., Polyakov, A., Nikiforov, V. & Goldfarb, A. (1994) *Proc. Natl. Acad. Sci. USA* **91,** 12036–12040.
35. Helm, K. v. d. & Krakow, J. S. (1972) *Nature New Biol.* **235,** 82–83.
36. Cassani, G., Burgess, R. R., Goodman, H. M. & Gold, L. (1971) *Nature New Biol.* **230,** 197–200.
37. Joyce, C. M. & Steitz, T. A. (1994) *Annu. Rev. Biochem.* **63,** 777–822.
38. Dieci, G., Hermann-Le Denmat, S., Lukhtanov, E., Thuriaux, P., Werner, M. & Sentenac, A. (1995) *EMBO J.* **14,** 3766–3776.
39. Orlova, M., Newlands, J., Das, A., Goldfarb, A. & Borukhov, S. (1995) *Proc. Natl. Acad. Sci. USA* **92,** 4596–4600.
40. Rudd, M. D., Izban, M. G. & Luse, D. S. (1994) *Proc. Natl. Acad. Sci. USA* **91,** 12036–12040.